Time-Dependent Laser Cavity Perturbation Theory: Exploring Future Nano-Structured Photonic Devices in Semi-Analytic way

Mariusz Drong, Maciej Dems, Jan Peřina Jr., Tibor Fördös, Henri-Yves Jaffrès, Kamil Postava, and Henri-Jean Drouhin

***Abstract*—We present a theoretical framework, which successfully combines two different fields of photonics: i) the laser rate equations and ii) the cavity perturbation theory, focusing particularly on micro-cavity lasers with optical anisotropies. Our approach is formally analogous to quantum-mechanical time-dependent perturbation theory, in which however the gain medium and permittivity tensor distribution are perturbed instead of the Hamiltonian. Using the general vectorial Maxwell-Bloch equations as a starting point, we derive polarization-resolved coupled-mode equations, in which all relevant geometric and anisotropy-related laser parameters are imprinted in its coefficients. Closed-form coupled-mode equations offer physical insights like rate equations approaches and the precision comparable to brute-force numeric routines, thus being the time-saving alternative to finite-difference time-domain methods. The main advantage is that one calculates numerically the shapes of cold-cavity modes used to derive coupled-mode equations for one set of parameters and the broad landscape of parameters of interest is further studied in a perturbative way. This makes the method particularly interesting for semi-analytic studies of state-of-art devices such as the photonic crystal lasers, the liquid-crystal lasers or specifically spin-lasers, in which the interplay between injected spin and cavity birefrigence creates very promising platform for ultrafast data transfer technologies.**

***Index Terms*—Anisotropies, cavity perturbation theory, micro-cavity lasers, polarization dynamics, rate equations.**

Manuscript received October 29, 2021; revised March 18, 2022; accepted April 6, 2022. Date of publication April 19, 2022; date of current version July 16, 2022. This work was supported in part by Doctoral Grant Competition VŠB TU-Ostrava, under Grant CZ.02.2.69/0.0./0.0/19_073/0016945 within the Operational Programme Research, Development and Education, under Grant DGS/TEAM/2020-027 Novel sources of THz radiation based on spintronic effects, in part by IT4 Innovations National Supercomputing Center Path to Exascale under Grant CZ.02.1.01/0.0/0.0/16_013/0001791, and in part by the Horizon 2020 Framework Programme of the European Commission under FET-Open Grant 863155 (s-Nebula). *(Corresponding author: Mariusz Drong.)*

Mariusz Drong is with the LSI, CEA/DRF/IRAMIS, CNRS, École Polytechnique, Institut Polytechnique de Paris, 91128 Palaiseau, France, and also with the IT4Innovations and Faculty of Materials Science and Technology, VŠB-Technical University of Ostrava, 708 00 Ostrava-Poruba, Czech Republic (e-mail: mariusz.drong@vsb.cz).

Kamil Postava is with the IT4Innovations and Faculty of Materials Science and Technology, VŠB-Technical University of Ostrava, 708 00 Ostrava-Poruba, Czech Republic (e-mail: kamil.postava@vsb.cz).

Maciej Dems is with the Institute of Physics, Technical University of Lodz, 90-924 Lodz, Poland (e-mail: maciej.dems@p.lodz.pl).

Jan Peřina Jr. is with the Joint Laboratory of Optics of Palacký University and Institute of Physics of Academy of Sciences of the Czech Republic, Palacký University, 772 07 Olomouc, Czech Republic (e-mail: jan.perina.jr@upol.cz).

Tibor Fördös is with the IT4Innovations and Nanotechnology Centre, CEET, VŠB-Technical University of Ostrava, 708 00 Ostrava-Poruba, Czech Republic (e-mail: tibor.fordos@vsb.cz).

Henri-Yves Jaffrès is with the Unité Mixte de Physique CNRS/Thales and Université Paris-Saclay, 91767 Palaiseau Cedex, France (e-mail: henri.jaffres@cnrs-thales.fr).

Henri-Jean Drouhin is with the LSI, CEA/DRF/IRAMIS, CNRS, École Polytechnique, Institut Polytechnique de Paris, 91128 Palaiseau, France (e-mail: henri-jean.drouhin@polytechnique.edu).

Color versions of one or more figures in this article are available at https://doi.org/10.1109/JLT.2022.3168231.

Digital Object Identifier 10.1109/JLT.2022.3168231

I. Introduction

FROM the historical point of view, the interest in time-dependent semi-analytic modeling of lasers with possible anisotropies has its origin in gas lasers, in which the major source of anisotropy is the lifting of atomic degeneracies due to external magnetic field. The first quantitative treatment was provided by Doyle *et al.* [1], building upon the revolutionary semi-classical laser theory of Lamb [2]. The novelty was based on respecting vectorial nature of electric field and assuming a possible non-collinearity between the electric field vector and the induced dipole moment density of active atoms. Additionally, the distributed loss anisotropy was included in the diagonal conductivity tensor. More detailed analysis, allowing to consider more general cavity anisotropies, was performed for a single-mode oscillation regime by van Haeringen *et al.* [3] and later for a multimode regime by Sargent *et al.* [4], [5], providing the theoretical background for the so-called Zeeman lasers. Alternative theory, including openness of laser resonators and allowing for a more complex field shapes, is due to Lenstra [6]. A simplified, and easier to work with, formalism based on studying the time evolution of Stokes vector of a laser beam was introduced by Tratnik *et al.* [7], [8]. More recently, Paddon *et al.* showed, how to evaluate the so-called anisotropy rates in laser rate equations in a simple round-trip model using the Jones matrix algebra [9].

Particularly rich analysis of polarization dynamics was performed for vertical-cavity surface-emitting lasers (VCSELs). A very successful spin-flip model (SFM), including electron spin degree of freedom, derived by San-Miguel *et al.* is still being used to study effects of in-plane phase and amplitude anisotropies in VCSELs [10], [11]. A very similar theory of Travagnin *et al.* is suitable for the description of non-collinearity of birefringence and dichroism principal axes [12], [13]. The

generalized SFM with a realistic variation of the gain on spin carrier concentrations was used to explain the polarization switching [14]. A weak point of SFM is that it cannot describe the geometric complexity of VCSEL cavities in a self-consistent way and the local nature of anisotropies [15], [16]. This was improved by the spatio-temporal models for VCSELs, which could partially account for the local anisotropies, the realistic gain variation with carrier concentration, the lateral dimensions of devices and the carrier diffusion [17], [18]. More recently, the index-guiding effects and transverse mode dynamics have been studied using generalized SFM with anisotropy rates extracted from the stationary wave equation, but for a simplified effective structure [19], [20].

None of the above-mentioned models can simultaneously describe any local anisotropies in both gain and passive media, the standing-wave cavity of arbitrary shape, out-of plane polarization or multiple-transition gain medium beyond 2-level atom approximation. In this paper, we adress this issue by deriving a polarization-dependent model which consistently combines the rate equations with cavity perturbation theory. Our approach can be understood as time-dependent perturbation theory, where the gain media properties, permittivity tensor distribution and to some extent the shape of the resonator can be perturbed instead of Hamiltonian and the effects consequently studied semi-analytically *via* explicitly formulated rate equations. For example, in contrast with Refs. [17], [18], the theory gives systematic theory of anisotropy rates. It is a direct polarization-dependent extension to the mathematical treatment of Hodges *et al.* [21]–[24], in which, however, we neglect the quantum noise. Our formulation does not assume any specific spatial dependence of vector eigen-mode basis functions as in the case of Hodges *et al.* Moreover, we propose a method how to treat the gain media with the general dependence of the susceptibility on population inversion (carrier concentration). The present work can be understood as direct generalization of Ref. [25], in which we describe spin-VCSELs with local anisotropies for ultrafast applications, while providing more rigorous basis for SFM.

The paper is organized in the following way: Section II introduces the general semi-classical Maxwell-Bloch theory of lasers with local anisotropies and multiple laser transitions with generally different polarization characteristics and frequency. In Section III, we provide the revisited recipe to derive polarization-resolved coupled-mode equations. This is followed by detailed analysis of anisotropy rates in Section IV, where the treatment is extended to include basis functions with different frequencies and the direct connection to the cavity perturbation theory is shown. The formalism is numerically validated in Section V by extracting the threshold modes of a pillar microcavity laser and comparing the results to fully-vectorial 2.5-D calculation. Moreover, we use our theory to uncover non-Hermitian physics of such structures, related to non-trivial polarization dynamics. Then, Appendix A shows new aspects of the theory of loss field. In Appendix B, we re-formulate the anisotropy operator. Finally, we show in Appendix C, how to apply this formalism to the cases in which the standard two-level atom approximation is not valid.

II. Maxwell-Bloch Equations for Anisotropic Lasers with Multiple Transitions

The derivation of coupled-mode equations is based on the standard semi-classical Maxwell-Bloch theory, describing the ensemble of quantum-mechanical two-level systems coupled to classical electromagnetic field *via* electric dipole interaction. We consider generally multiple laser transitions labeled by μ, each having their own emission energy and polarization characteristics. Polarization-dependent gain is described by the gain tensor $\hat{\mathcal{T}}_\mu(\mathbf{r})$ [26]. Spatially-dependent optical anisotropies of a laser cavity are self-consistently included in the relative permittivity tensor $\hat{\varepsilon}(\mathbf{r},\omega)$ of background passive media. After having employed the rotating-wave approximation (RWA) with respect to frequency ω, we derive the modified Maxwell-Bloch equations that couple the dipole moment densities $\tilde{\mathbf{P}}_\mu(\mathbf{r},t)$, population inversions $N_\mu(\mathbf{r},t)$ and the complex electric field amplitude $\mathbf{E}(\mathbf{r},t)$ [27]–[29]:

$$\begin{aligned}\frac{\partial}{\partial t}\tilde{\mathbf{P}}_\mu(\mathbf{r},t) = &-(\gamma_{\perp,\mu}+i\Delta_\mu)\,\tilde{\mathbf{P}}_\mu(\mathbf{r},t)\\ &+\frac{i}{\hbar}|\theta_\mu|^2 N_\mu(\mathbf{r},t)\hat{\mathcal{T}}_\mu(\mathbf{r})\mathbf{E}(\mathbf{r},t),\end{aligned} \tag{1}$$

$$\begin{aligned}\frac{\partial}{\partial t}N_\mu(\mathbf{r},t) = &-\gamma_{\parallel,\mu}\,N_\mu(\mathbf{r},t)+\Lambda_\mu(\mathbf{r},t)\\ &+\frac{2i}{\hbar}\left[\mathbf{E}^\dagger(\mathbf{r},t)\tilde{\mathbf{P}}_\mu(\mathbf{r},t)-\text{c.c.}\right],\end{aligned} \tag{2}$$

$$\begin{aligned}&\left[c^2\nabla^2-\hat{\varepsilon}(\mathbf{r},\omega)\frac{\partial^2}{\partial t^2}-\frac{\zeta(\mathbf{r},\omega)}{\varepsilon_0}\frac{\partial}{\partial t}\right]\mathbf{E}(\mathbf{r},t)\exp(i\omega t)\\ &\qquad=\frac{1}{\varepsilon_0}\frac{\partial^2}{\partial t^2}\sum_\mu\tilde{\mathbf{P}}_\mu(\mathbf{r},t)\exp(i\omega t),\end{aligned} \tag{3}$$

where $\gamma_{\perp,\mu}$, Δ_μ, $\hbar$ and θ_μ are the dipole moment relaxation coefficient, spectral detuning, Dirac constant and the magnitude of electric dipole moment operator off-diagonal matrix element, respectively. The incoherent processes of the population inversion $N_\mu(\mathbf{r},t)$ are described by decay coefficient $\gamma_{\parallel,\mu}$ and pumping rate $\Lambda_\mu(\mathbf{r},t)$. Any losses originating from an intra-cavity absorption or cavity leakage are given by the phenomenological conductivity $\zeta(\mathbf{r},\omega)$. Note, that the total electric field intensity is $\mathbf{F}(\mathbf{r},t)=\mathbf{E}(\mathbf{r},t)\exp(i\omega t)+\text{c.c.}$ and the complex dipole moment density $\tilde{\mathbf{P}}_\mu(\mathbf{r},t)$ contributes to the total complex dipole moment density as $\mathbf{P}(\mathbf{r},t)=\mathbf{P}_b(\mathbf{r},t)+\sum_\mu\tilde{\mathbf{P}}_\mu(\mathbf{r},t)$, where $\mathbf{P}_b$ is the dipole moment density of the background non-lasing media.

III. Polarization-Resolved Coupled-Mode Theory

A. The principle

In the following, we construct the polarization-resolved extension to the formalism of Hodges *et al.* [21]. It is assumed, that the laser field consists of a certain number of simultaneously-oscillating modes of given frequency and polarization. The

coupled-mode equations are derived by projecting the Maxwell-Bloch equations onto the general eigen-mode system and performing integration over the entire volume of the laser cavity. Thus, one obtains the set of time-dependent coupled ordinary differential equations. It means, that the cavity geometry and optical-anisotropic parameters are effectively imprinted into the coefficients of those differential equations. Very similar approach adopt also recently very successful *Steady-state ab-initio lasing theory* (SALT), which can also describe complex cavity geometries, local anisotropies and multiple transitions. However, SALT deals only with steady-state lasing [30]–[32]. In this view, our formalism can be considered the time-dependent counterpart of single-pole approximation SALT (SPA-SALT).

A particular focus is paid to the role of local anisotropies of the gain medium and passive cavity anisotropies, which give rise to so-called anisotropy rates. According to Appendix B, the passive cavity anisotropies are included in anisotropy operator $\hat{\gamma}(\mathbf{r},\omega) = i(\omega/2)\hat{\varepsilon}(\mathbf{r},\omega) + i(c^2/2\omega)\hat{1}\nabla^2$ (with $\hat{1}$ being the unity operator), which is the function of $\hat{\varepsilon}(\mathbf{r},\omega)$ (in the case of degenerate-frequency basis functions, as done in Ref. [25], here the theory is extended) and which is mostly completely neglected in the isotropic treatment, because its terms disappear when the slowly-varying envelope approximation (SVEA) in the space domain is employed. Such term allows for example to include the corrections as in cavity perturbation theory.

The standard decomposition for complex electric field amplitude is written as:

$$\mathbf{E}(\mathbf{r},t) = \sum_k E_k(t)\boldsymbol{\varphi}_k(\mathbf{r})\exp(i\delta\omega_k t), \tag{4}$$

where $\boldsymbol{\varphi}_k(\mathbf{r})$ are the vectorial eigen-mode spatial functions which can be extracted specifically for each laser cavity by robust numeric methods such as the finite element/difference methods or specifically the plane-wave admittance method (PWAM), which is used within this paper. We neglect relative phase shifts, because laser applications such as mode-locking are not considered here. Eigen-mode frequencies ω_k are generally shifted by $\delta\omega_k$ with respect to the reference frequency ω. The effects of cavity anisotropy can be included directly in $\boldsymbol{\varphi}_k(\mathbf{r})$ for simple cases, however generally they are treated as cavity perturbation $\delta\hat{\varepsilon}(\mathbf{r},\omega) = \hat{\varepsilon}(\mathbf{r},\omega) - \varepsilon(\mathbf{r},\omega)\,\hat{1}$, where $\varepsilon(\mathbf{r},\omega)$ is assumed to be the real part of the diagonal element of isotropic relative permittivity tensor, since the losses can be included in $\zeta(\mathbf{r},\omega)$. Note, that the perturbation $\delta\hat{\varepsilon}(\mathbf{r},\omega)$ can be complex, in general.

The working principle of our approach can be summarized as shown in Fig. 1: i) a particular set of eigen-mode functions, with generally different frequencies and polarizations (we prefer linearly-polarized functions here for particular analytic calculations) is extractd and ii) the equations of motion for amplitudes $E_k(t)$ expressed using such eigen-modes are derived (including population inversion and dipole moment density), iii) the effects of the cavity geometry, mode coupling and most-importantly the anisotropies are included in the appropriate coefficients. It is worth noting, that our approach shares similarities with the temporal coupled-mode theory for the analysis of coupled waveguides and includes cavity perturbation theory. This suggests that the advantage, compared to robust numerical methods [33] is that one calculates numerically the shapes of eigen-mode functions for one set of parameters and the broad landscape of parameters of interest is further studied analytically in a perturbative way.

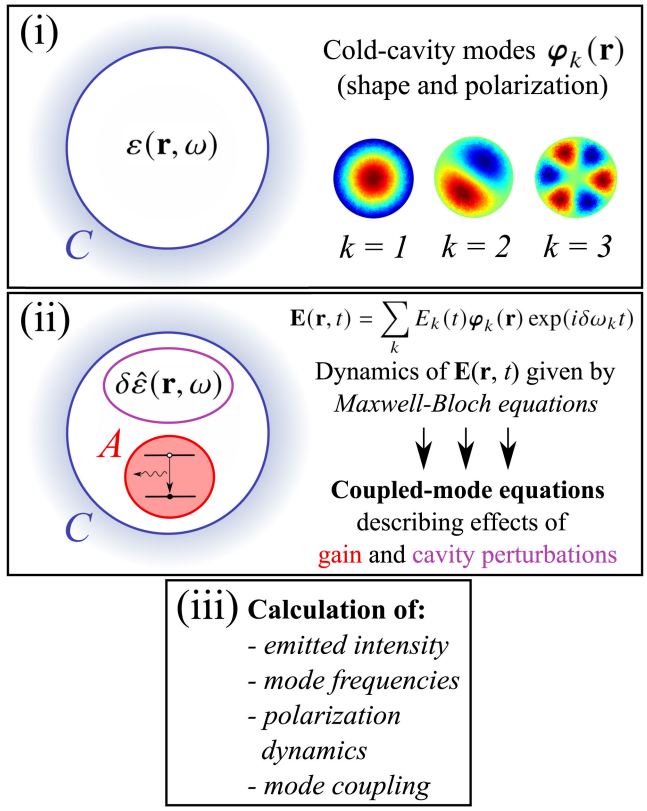

Fig. 1. A working principle of the formalism consisting of three steps: (i) numerical extraction of cold-cavity modes including polarization state, (ii) derivation of coupled-mode equations describing the effects of gain medium and cavity perturbations such as local anisotropies and (iii) calculation of important observables such as time-dependent polarization state or coupling between modes.

B. Quasi-Hermitian basis

Let us now define the basis of cold-cavity modes, in which the dipole moment density and electric field amplitude will be decomposed:

$$|\tilde{P}_\mu(t)\rangle = \sum_k \tilde{P}_{\mu,k}(t)|k\rangle\exp(i\delta\omega_k t),$$
$$|E(t)\rangle = \sum_k E_k(t)|k\rangle\exp(i\delta\omega_k t), \tag{5}$$

where we employ the bra-ket notation for cold-cavity modes $|k\rangle$ in the following sense $\boldsymbol{\varphi}_k(\mathbf{r}) = \langle\mathbf{r}||k\rangle$. The coefficients of the decomposition $\tilde{P}_{\mu,k}(t)$ and $E_k(t)$ stands for the time-depentent dipole moment densities and electric field amplitudes and $\delta\omega_k$ are the frequency shifts with respect to reference frequency ω. Since we consider 'good cavities' with high Q-factor, the

orthogonality relations hold:

$$\langle j|\varepsilon(\mathbf{r},\omega)|k\rangle_C = \int_C \boldsymbol{\varphi}_j^\dagger(\mathbf{r})\varepsilon(\mathbf{r},\omega)\boldsymbol{\varphi}_k(\mathbf{r})\,d^3\mathbf{r} \approx \delta_{jk}\,\mathcal{C}_k, \tag{6}$$

where C stands for the integration over entire cavity volume. On the other hand, the orthogonality of modes within the active medium is rarely satisfied, thus we define the overlaps:

$$\langle j|k\rangle_A = \mathcal{A}_{jk}, \tag{7}$$

where A stands for the integration over the active region.

C. Coupled-mode equations

1) Electric field amplitudes: In order to derive the equations of motion for electric field amplitudes, we will decompose the original wave equation into particular modes and finally perform SVEA to get rid of second-order time derivatives, as originally done by Hodges *et al.* for isotropic case [21], [22]. Employing (5), multiplying the (3) by $\langle j|$ and using the orthogonality relations together with SVEA in the time-domain, we obtain the equation of motion for $E_j(t)$:

$$\begin{aligned}\frac{d}{dt}E_j(t) = &-\kappa_j E_j(t)\\ &- i\frac{\omega_j}{2\varepsilon_0}\frac{1}{\mathcal{C}_j}\sum_{\mu;k}\mathcal{A}_{jk}\tilde{P}_{\mu,k}(t)f_{kj}(t)\\ &-\sum_k \gamma_{jk}\,E_k(t)\,f_{kj}(t),\end{aligned} \tag{8}$$

where the field decay rate κ_j is defined as:

$$\kappa_j = \frac{1}{2}\frac{\langle j|\tilde{\kappa}(\mathbf{r},\omega_j)|j\rangle}{\langle j|\varepsilon(\mathbf{r},\omega_j)|j\rangle} \tag{9}$$

and the local loss field $\tilde{\kappa}(\mathbf{r},\omega_j) = \zeta(\mathbf{r},\omega_j)/\varepsilon_0$ is introduced as in Appendix A. The beating term $f_{kj}(t) = \exp[i(\delta\omega_k - \delta\omega_j)t]$ is defined, for which $f_{jk}(t) = [f_{kj}(t)]^*$ applies. Frequencies $\omega_j = \omega + \delta\omega_j$ are the absolute frequencies of laser modes.

Most importantly, the generalized anisotropy rate γ_{jk} has been derived:

$$\gamma_{jk} = i\left(\frac{\omega_k}{\omega_j}\right)^2\frac{\omega_j}{2}\frac{\langle j|\delta\hat{\varepsilon}(\mathbf{r},\omega_j)|k\rangle}{\langle j|\varepsilon(\mathbf{r},\omega_j)|j\rangle}. \tag{10}$$

Such expression represents a generalization of the concept of anisotropy operator $\hat{\gamma}(\mathbf{r},\omega)$ from Ref. [25], which was however suitable only for basis functions with no separation of frequencies. Furthermore, it is suitable for the vector basis functions of any spatial dependence of the polarization vector.

2) Dipole moment density: Employing (5), multiplying the (1) by $\langle j|$ and using the orthogonality relations, we obtain the equation of motion for $\tilde{P}_{\mu,j}(t)$:

$$\begin{aligned}\frac{d}{dt}\tilde{P}_{\mu,j}(t) = &-\beta_{\mu,j}\tilde{P}_{\mu,j}(t)\\ &+\frac{i}{\hbar}|\theta_\mu|^2\sum_{k,l}(\mathcal{A}^{-1})_{jk}\mathcal{N}_\mu^{kl}(t)\,E_l(t)\,f_{lj}(t),\end{aligned} \tag{11}$$

where we define $\beta_{\mu,j} = \gamma_{\perp,\mu} + i(\Delta_\mu + \delta\omega_j)$. Note again, that the active medium background permittivity $\varepsilon_a(\omega_j)$ is assumed to be constant within its volume.

For the general cases, in which for example the anisotropic properties of the gain medium depend on position, we have to define population inversion overlaps as:

$$\mathcal{N}_\mu^{kl}(t) = \langle k|N_\mu(\mathbf{r},t)\,\hat{\mathcal{T}}_\mu(\mathbf{r})|l\rangle, \tag{12}$$

for which it is necessary to find the equations of motion.

3) Population inversion overlaps: In order to satisfy the definition of $\mathcal{N}_\mu^{jk}(t)$, one has to act on both sides of the (2) using $\langle j|(...)\,\hat{\mathcal{T}}_\mu(\mathbf{r})|k\rangle$ to obtain:

$$\begin{aligned}\frac{d}{dt}\mathcal{N}_\mu^{jk}(t) = &-\gamma_{\parallel,\mu}\mathcal{N}_\mu^{jk}(t) + \Lambda_\mu^{jk}(t)\\ &-\frac{4}{\hbar}\sum_{l,m}\mathrm{Im}\left\{E_l^*(t)\mathcal{W}_{\mu,lm}^{jk}\tilde{P}_{\mu,m}(t)f_{ml}(t)\right\},\end{aligned} \tag{13}$$

where the coupling coefficients $\mathcal{W}_{\mu,lm}^{jk}$ have been defined:

$$\mathcal{W}_{\mu,lm}^{jk} = \langle j|\hat{\mathcal{T}}_\mu(\mathbf{r})\langle l|\delta_{\mathbf{rr}'}|m\rangle|k\rangle, \tag{14}$$

where $\delta_{\mathbf{rr}'}$ stands for the Dirac delta function $\delta(\mathbf{r}-\mathbf{r}')$, where $\mathbf{r}'$ denotes coordinates of all points within the active medium.

(8), (11) and (13) form the general mathematical framework for the analysis of the polarization dynamics of lasers involving a broad range of cavity geometries and optical-anisotropic properties. Note, that even though (8), (11) and (13) seem to be rather complicated, for the most of the practical applications they can be significantly simplified, as shown in Section V.

IV. Theory of Anisotropy Rates: Consistency with 1st-Order Cavity Perturbation Theory

A. General analytic formulas

In this part we re-formulate and generalize the theory of anisotropy rates. Previously, the analysis was restricted to two transverse modes of the same frequency, which is extended here. A general anisotropy rate is defined according to (10) and can be applied to the numeric evaluation using eigen-mode functions of any spatial and polarization dependence. Although, in principle, the theory allows to describe any experimental situations, we limit our considerations to the cases, in which it is possible to separate spatial and polarization part of eigen-mode functions, in order to obtain simple analytic formulas. Moreover, we assume the use of a set of linearly-polarized eigen-mode functions.

Once we assume the separability of $|j\rangle = \mathbf{e}_j|\varphi]$, (10) becomes:

$$\gamma_{jk} = i\left(\frac{\omega_k}{\omega_j}\right)^2 \frac{\omega_j}{2} \sum_n \Gamma_{jk,n} \mathbf{e}_j^\dagger \, \delta\hat{\varepsilon}_n(\omega_j)\, \mathbf{e}_k, \tag{15}$$

where the generalized confinement factor has been defined:

$$\Gamma_{jk,n} = \frac{[j|k]_n}{[j|\varepsilon(\mathbf{r},\omega_j)|j]_C}. \tag{16}$$

Note that summation (over n) represents the fact, that the laser can contain several anisotropic media, as for example not homogeneously strained layers in the vertical-cavity lasers [34], studied in detail for example in Ref. [16]. The result is very intuitive and expresses the fact that the anisotropy rate is proportional to the number of field oscillations per unit of time, the fraction of electromagnetic energy confined within anisotropic domain and the polarization overlap of the given permittivity perturbation.

B. Frequency-degenerate polarization modes and in-plane anisotropy perturbation

As a special case, we consider modes of the same frequency but characterized by orthogonal polarization. This means to take $\delta\omega_k \to 0$, i.e. $\omega_k \to \omega$ and reduce the confinement factor to $\Gamma_{jk,n} \to \Gamma_n$. Equation (15) then reduces to:

$$\gamma_{jk} = i\,\frac{\omega}{2} \sum_n \Gamma_n \, \mathbf{e}_j^\dagger \, \delta\hat{\varepsilon}_n(\omega)\, \mathbf{e}_k. \tag{17}$$

For simplicity, we consider frequency-degenerated linearly-polarized eigen-mode functions and the following reduced permittivity tensor of nth cavity domain, describing a general in-plane anisotropies:

$$\hat{\varepsilon}_n = \begin{bmatrix} \varepsilon_n + \delta\varepsilon_{n,xx} & \delta\varepsilon_{n,xy} \\ \delta\varepsilon_{n,yx} & \varepsilon_n + \delta\varepsilon_{n,yy} \end{bmatrix}. \tag{18}$$

Using (17), we derive:

$$\gamma_{jk} = i \sum_n \Gamma_n \left(\frac{\omega}{2}\right) \delta\varepsilon_{n,jk}, \tag{19}$$

where it should be noted, that $\delta\varepsilon_{n,jk}$ can be composed of real and imaginary parts.

1) Linear birefringence and dichroism: Let us now consider the particular case of a linear anisotropy:

$$\hat{\varepsilon}_n = \begin{bmatrix} \varepsilon_n + \delta\varepsilon_{n,x} & 0 \\ 0 & \varepsilon_n + \delta\varepsilon_{n,y} \end{bmatrix}, \tag{20}$$

where the anisotropy perturbation $\delta\varepsilon_{n,j}$ consists of a real and an imaginary parts $\delta\varepsilon_{n,j} = \delta\varepsilon_{n,j}^r - i\delta\varepsilon_{n,j}^i$, which models linear birefringence and linear dichroism, respectively. All the elements of permittivity tensors are evaluated at the frequency ω. The calculation leads to:

$$\gamma_{jj} = i \sum_n \Gamma_n \left(\frac{\omega}{2}\right) \delta\varepsilon_{n,j}, \tag{21}$$

where the real part represents the dichroism rate $\gamma_{a,j}$, used in SFM of VCSELs, and the imaginary part is the birefringence rate $\gamma_{p,j}$. If one makes the following symmetric choice for the perturbation terms: $\delta\varepsilon_{n,x}^r = -\delta\varepsilon_{n,y}^r = \delta\varepsilon_n^r/2$ and $\delta\varepsilon_{n,x}^i = -\delta\varepsilon_{n,y}^i = -\delta\varepsilon_n^i/2$, the resulting expressions are equivalent to those in Ref. [25], obtained using circularly-polarized eigen-mode functions. Additionally, with such choice of perturbation terms, one obtains the symmetric anisotropy rates γ_a, γ_p of San Miguel *et al.* [10], [11].

2) Circular anisotropies in polar configuration: Similar analytic expressions can be derived for any other type of anisotropy. Here we choose the circular anisotropy, such as those of polar magneto-optic configurations. Let us have the following permittivity tensor:

$$\hat{\varepsilon}_n = \begin{bmatrix} \varepsilon_n & i\xi_n \\ -i\xi_n & \varepsilon_n \end{bmatrix}, \tag{22}$$

where ξ_n can be considered as a magneto-optic perturbation of the permittivity tensor. Using again the frequency-degenerated linearly-polarized eigen-mode functions, we obtain the off-diagonal rates:

$$\gamma_{xy} = -\gamma_{yx} = -\sum_n \Gamma_n \left(\frac{\omega}{2}\right) \xi_n. \tag{23}$$

C. The direct connection to cavity perturbation theory

In principle, the perturbation $\delta\varepsilon(\mathbf{r},\omega) = \delta\varepsilon_r(\mathbf{r},\omega) + i\delta\varepsilon_i(\mathbf{r},\omega)$ does not have to be represented by a matrix form. It can be the scalar perturbation of the cavity media permittivity and we are now going to demonstrate the direct connection with the cavity perturbation theory [35].

Let us consider the oscillation of a single mode of amplitude $E_j(t)$ with compensated gain and loss. The equation of motion is:

$$\frac{d}{dt}E_j(t) = -\gamma_{jj}E_j(t), \tag{24}$$

where the diagonal anisotropy rate reads:

$$\gamma_{jj} = i\frac{\omega_j}{2}\frac{\langle j|\delta\varepsilon_r(\mathbf{r},\omega_j)|j\rangle_C}{\langle j|\varepsilon(\mathbf{r},\omega_j)|j\rangle_C} - \frac{\omega_j}{2}\frac{\langle j|\delta\varepsilon_i(\mathbf{r},\omega_j)|j\rangle_C}{\langle j|\varepsilon(\mathbf{r},\omega_j)|j\rangle_C}. \tag{25}$$

The integration is performed over the entire mode volume. The consequence of the real part $\delta\varepsilon_r(\mathbf{r},\omega_j)$ is that the oscillations of $E_j(t)$ are shifted due to the imaginary part of γ_{jj}, which is equal to $\Delta\omega_j$ and its relative value may be expressed as:

$$\frac{\Delta\omega_j}{\omega_j} = -\frac{1}{2}\frac{\langle j|\delta\varepsilon_r(\mathbf{r},\omega_j)|j\rangle_C}{\langle j|\varepsilon(\mathbf{r},\omega_j)|j\rangle_C}. \tag{26}$$

This is in agreement with the basic result of the first-order cavity perturbation theory [35]. On the other hand, the imaginary part of perturbation $\delta\varepsilon_i(\mathbf{r},\omega_j)$ leads to change of cavity decay rate κ_j as $\kappa_j + \Delta\kappa_j$. The sign of $\delta\varepsilon_i(\mathbf{r},\omega_j)$ determines, if the losses are increased or decreased. Note, that the generalization to quasi-normal modes is straightforward.

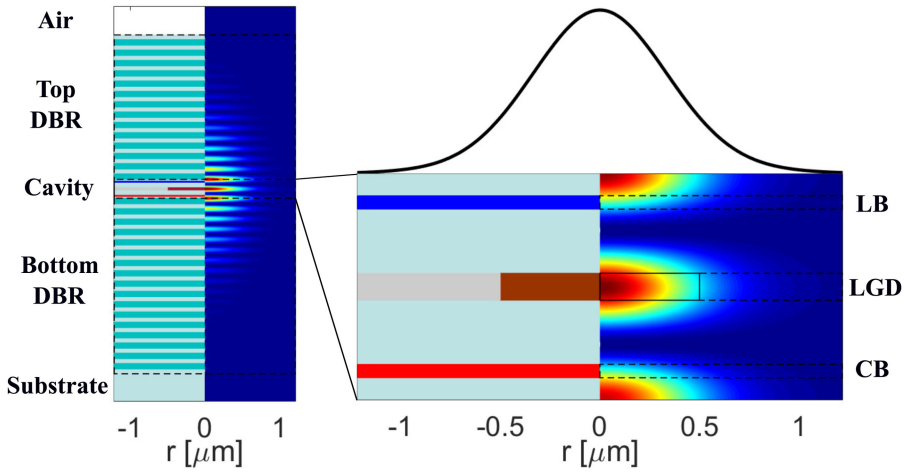

Fig. 2. Fundamental mode of the unperturbed (isotropic) pillar microcavity laser structure with a single active layer enclosed within two DBRs, emitting to the air. Inset shows a detailed composition of the cavity, consisting of layers, which are to be perturbed by the linear (LB, blue layer) and circular (CB, red layer) birefringence, and active layer with 1 μm aperture and linear gain dichroism (LGD, brown layer). Schemes are symmetrically divided to show the laser geometry as well as the field distribution at once.

V. Numerical Validation: Fundamental Polarization Modes of Pillar Microcavity Laser

In this section we use our formalism to calculate the measurable quantities of specific laser structure, depending mainly on local optical anisotropies. Namely, we calculate the frequency difference, the ratio of population inversions and polarization states of two lowest-order threshold modes of pillar microcavity laser, which is shown in Fig. 2. The structure is not supposed to represent the realistic device, it is meant to be used only for the numerical validation of our formalism.

A. The structure

The radially-symmetric laser consists of the short cavity of permittivity $\varepsilon = 9$, with a single active layer with 1 μm aperture made of $\varepsilon = 4$ material and thickness $d = 40$nm. The background (passive) permittivity of active layer is the same as of the cavity and additionally we consider linear gain dichroism as an adjustable parameter of active layer. The longitudinal optical confinement is ensured by two DBRs with 14 and 17 pairs of $\varepsilon = 9$ and $\varepsilon = 6.25$ materials, having thicknesses $d = 83.3$ nm and $d = 100$ nm, respectively. The structure is grown on a $\varepsilon = 9$ substrate and is emitting into the air at free-space wavelength $\lambda = 987$ nm. The height of an entire pillar is about 6 μm. Furthermore, the cavity contains 2 layers with linear and circular birefringence as an adjustable parameters. Both potentially anisotropic layers have thickness $d = 20$ nm and background permittivity $\varepsilon = 9.61$ and $\varepsilon = 8.41$, respectively. In the unperturbed (isotropic) state, the cold-cavity has a quality-factor $Q = 2322.36$, which was calculated using the plane-wave admittance method (PWAM), and which corresponds to the photon lifetime $\tau_{ph} = 1.216$ps.

The optical-material anisotropies are introduced as perturbations to the isotropic background permittivity, generally as $\hat{\varepsilon}_j = \varepsilon_j \hat{1} + \delta\hat{\varepsilon}_j$. Concerning the layer with the linear birefringence, the anisotropic perturbation takes the diagonal form: $\delta\hat{\varepsilon}_{LB} = \mathrm{diag}(\delta_l, -\delta_l)/2$, where δ_l as a real number. In the case of circularly birefringent layer, it is: $\delta\hat{\varepsilon}_{CB} = \text{off-diag}(i\delta_c, -i\delta_c)/2$, where δ_c is also a real number. The linear gain dichroism of active layer is quantified using so-called gain tensor $\hat{\mathcal{T}} = \mathrm{diag}(1+\delta_g, 1-\delta_g)$, where δ_g is a real number, as well.

B. Rate equations

Let's assume, that the considered pillar microcavity laser is a class-B laser, as indicated by the calculated photon lifetime, which is in the ps-range. Consequently, we can adiabatically eliminate dipole moment density. Moreover, the resulting equations will be simplified when using:

$$|E(t)\rangle = [E_x(t)\,\mathbf{e}_x + E_y(t)\,\mathbf{e}_y]|\varphi]. \tag{27}$$

Namely, the terms $f_{kj}(t)$ disappear and spatial overlaps reduce to $\mathcal{A} = [\varphi|\varphi]_A$, $\mathcal{C} = [\varphi|\varepsilon(\mathbf{r},\omega)|\varphi]_C$ and $\mathcal{W} = [\varphi|[\varphi|\delta_{\mathbf{rr}'}|\varphi]|\varphi]_A$, respectively. Moreover, we can simply approximate the population inversion as $N(\mathbf{r},t) = \mathcal{N}(t)\,\phi(\mathbf{r})$ where the spatial part takes the value $\phi(\mathbf{r}) = 1$ in the active region and $\phi(\mathbf{r}) = 0$ otherwise, due to well-localized electronic wave functions in QWs. One then derives:

$$\frac{d}{dt}A_j(t) = \kappa\left[\Gamma\, n(t)\,\mathcal{T}_j - 1\right] A_j(t) - \sum_k \gamma_{jk} A_k(t), \tag{28}$$

$$\frac{1}{\gamma_\parallel}\frac{d}{dt}n(t) = n_0(t) - \left\{1 + \tilde{\Gamma}\sum_k \left[\mathcal{T}_k |A_k(t)|^2\right]\right\} n(t), \tag{29}$$

for re-scaled variables $A_j(t)$ and $n(t)$, defined as: $E_j(t) = \frac{\hbar}{2|\theta|}\sqrt{\gamma_\perp\gamma_\parallel}\,A_j(t)$ and $\mathcal{N}(t) = \frac{2\hbar\varepsilon_0}{|\theta|^2\omega}\gamma_\perp\kappa\, n(t)$, respectively. It is assumed there, that the active medium is tuned exactly at cavity resonance, which gives $\Delta = 0$. The confinement factors are defined as $\Gamma = \mathcal{A}/\mathcal{C}$ and $\tilde{\Gamma} = \mathcal{W}/\mathcal{A}$ and where $\mathcal{T}_j = \mathbf{e}_j^\dagger \hat{\mathcal{T}}\,\mathbf{e}_j$.

C. The threshold modes

1) Extraction of the threshold modes: In the following, we are interested only in the properties of the lowest-order threshold modes, namely their frequencies, population inversions (gains) and polarization states (Stokes vectors), while they depend mainly on anisotropies. Thus, we only need to solve (28). Expressed in the matrix form, for amplitudes $A_x(t)$ and $A_y(t)$ we have:

$$\frac{d}{dt}\mathbf{A}(t) = \hat{\mathcal{D}}(\kappa, n, \delta_g, \delta_l, \delta_c)\mathbf{A}(t). \tag{30}$$

The mathematical solution is:

$$\mathbf{A}(t) = \sum_{j=a,b} \alpha_j \, \mathbf{v}_j \exp(\eta_j t), \tag{31}$$

where $\mathbf{v}_j$ and η_j are the eigen-vectors and eigen-values of matrix $\hat{\mathcal{D}}$: $\hat{\mathcal{D}}\,\mathbf{v}_j = \eta_j\,\mathbf{v}_j$. The amplitudes $\alpha_{a,b}$ of two possible polarization modes a and b are not given absolutely, since the laser thresholds are considered. Note, that the polarization states of eigen-modes can be computed directly from eigen-vectors $\mathbf{v}_{a,b}$. On the other hand, the threshold population inversions $n^{th}_{a,b}$ are extracted from the solution of: $\mathrm{Re}\{\eta_j(n^{th}_j)\} = 0$. The frequency shifts of the given modes at the threshold are given directly by $\Delta\omega_j = \mathrm{Im}\{\eta_j(n^{th}_j)\}$.

2) The results: In order to show the precision of our formalism, we use the plane-wave admittance method (PWAM) as a reference [36]. It is a computational method combining the plane-wave expansion method with the method of lines (MoL), showing brilliant agreement with experimental data [37]. PWAM calculation also provides the shape of unperturbed degenerate fundamental cavity mode, which allows to calculate the necessary confinement factors $\Gamma = 0.0042$, $\Gamma_{\mathrm{LB}} = 0.00154$ and $\Gamma_{\mathrm{CB}} = 0.00187$ of active and anisotropic layers, respectively. It is worth noting, that we are comparing two entirely different approaches for modeling of lasers, especially that PWAM is intended for precise determination of static properties while our CMT for dynamical properties in the phenomenological rate-equation-like sense. However, the lack of computational self-consistency or predictability from the point of view of geometric and local material properties of lasers has always been a weak point of rate-equation-like approaches. This is, where we provide an improvement.

We compare the calculated frequency splitting $\Delta\nu = |\omega_a - \omega_b|/(2\pi)$, depending on linear (LB) and circular (CB) birefringence, in Fig. 3(a). The calculation shows a very good agreement with PWAM. In Fig. 3(b), we are showing the calculation of n^{th}_b/n^{th}_a ratio, achieving excellent match with PWAM results as well.

Additionally, we compare the numerically obtained Stokes vector's components $\mathbf{S}_1 = I_x - I_y$, $\mathbf{S}_2 = I_{45^\circ} - I_{-45^\circ}$, defined as intensity difference of linearly-polarized components along $\mathbf{x}/\mathbf{y}$ axes and axes rotated by 45°, respectively and $\mathbf{S}_3 = I_R - I_L$, defined as the intensity difference of circularly-polarized components. The results are depicted in Figs. 4(a) and (b) for two possible polarization modes a and b. Despite the fact, that the structure is only a toy-model for numerical validation, a similar situation can be observed in spin-VCSELs, in which the cavity linear birefringence competes with the circular gain dichroism of spin-injected QWs to determine the polarization states of modes [38]–[40]. Depending on the strengths of each anisotropy, the continuous polarization phase transition can take place going from purely linear, through elliptic to circular polarization, as the circular gain dichroism increases due to spin injection.

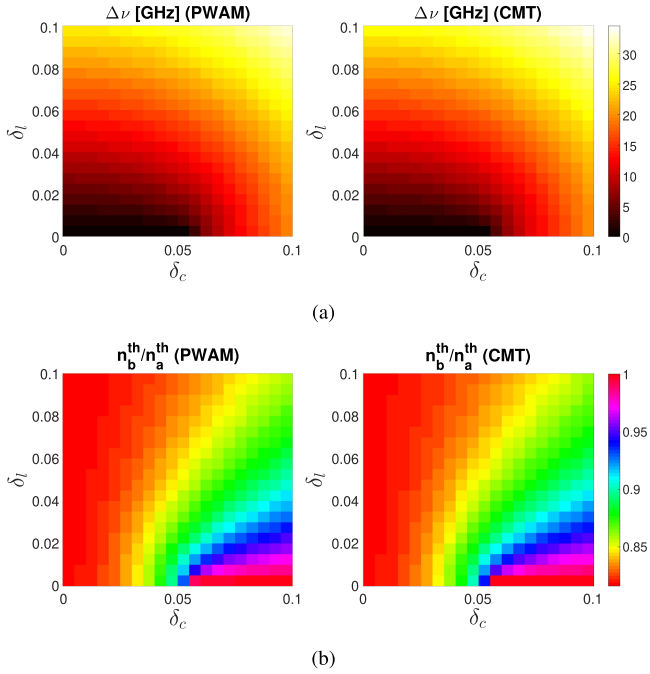

Fig. 3. Calculated (a) frequency splitting $\Delta\nu$ and (b) ratio of threshold populations n^{th}_b/n^{th}_a of two fundamental threshold modes of the pillar microcavity structure as function of linear (δ_l) and circular (δ_c) birefringence with fixed value of linear gain dichroism $\delta_g = 0.1$. The proposed coupled-mode theory (CMT) is compared to the robust plane-wave addmittance method (PWAM).

D. Time-Dependence of Optical Fields

Considering the micro-pillar laser in Fig. 2 with given parameters, one can expect typical ns-scale dynamics characteristic for class-B laser with strong relaxation oscillations. Moreover, multiple sources of anisotropy in the structure lead to very rich polarization dynamics. To demonstrate one such example, we show time traces of $A_{x,y}(t)$ and $n(t)$ in Fig. 5(a) obtained by solving numerically (28) and (29) taking $\delta_g = 0.1$, $\delta_l = 0$ and $\delta_c = 0.045$ with pumping rate n_0 twice above the threshold value, which is typically given by $n_{0,th} \approx \Gamma^{-1}$. In simulation, we used $\gamma_\parallel = 1\mathrm{ns}^{-1}$ and $\tilde{\Gamma} = 1$. Normally, the linear gain dichroism $\delta_g \neq 0$ alone would lead to emission of field polarized along $\mathbf{x}$ or $\mathbf{y}$ axis. In this case, however, the present circular anisotropy $\delta_c \neq 0$ couples two components $A_x(t)$ and $A_y(t)$. Note, that the reason to choose such specific values of anisotropies can be seen in Figs. 3(b), 4(a) and (b), where $\delta_l = 0$, $\delta_c = 0.045$ is close to the critical point of polarization 'phase transition' discussed previously. Such points are called the exceptional point (EP), typical for non-Hermitian systems [41]. They can be identified in Fig. 5(b). It can be shown, that the critical value of circular anisotropy is $\delta_c = \frac{2\,\delta_g\,\kappa}{\pi\Gamma_{CB}\,\nu} \approx 0.0509$, when

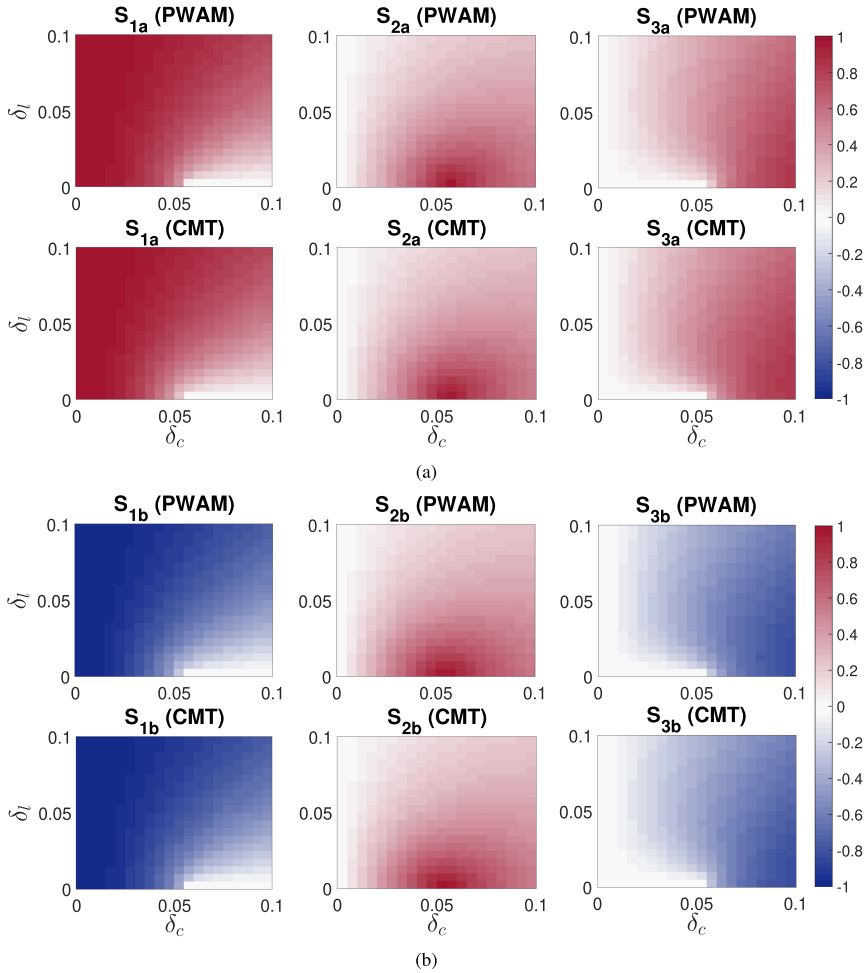

Fig. 4. Calculated Stokes vector components $\mathbf{S}_1$, $\mathbf{S}_2$ and $\mathbf{S}_3$ of threshold modes a (a) and b (b) as function of linear (δ_l) and circular (δ_c) birefringence with fixed value of linear gain dichroism $\delta_g = 0.1$. The proposed coupled-mode theory (CMT) is compared to the robust plane-wave admittance method (PWAM).

$\delta_l = 0$. For $\delta_g = 0.1$, $\delta_l = 0$ and approximately $\delta_c < 0.04$ the device reaches a steady-state. On the other hand, increasing to $\delta_c > 0.055$ (above EP) leads to $\pi/2$ - shifted oscillations of total $\mathbf{S}_{1,2}$ components, emitting effectively a circularly polarized field.

VI. Conclusion and Discussion

In this work we combine the laser rate equations with cavity perturbation theory to describe the polarization dynamics of lasers with local anisotropies and multiple optical transitions. The time-dependent theory is formulated for the standing-wave lasers with generally any cavity geometry and spatial dependence of anisotropies. The theory was used to predict the existence of EPs arising from polarization dynamics of anisotropic structures. Such system can be experimentally realized for example by micropillar lasers with strained active region and chiral metasurface on top DBR. It was shown, that the formalism is not limited by the standard two-level atom approximation. Additional effects such as nonlinear response of the gain medium can be included as well as coupling effects arising from the non-orthogonality of basis modes within the entire laser cavity.

Some of the relevant photonic structures, for which our semi-analytic formalism is already suitable in the present state or can be suitable after few improvements, are the microcavity photonic crystal lasers [22], [42], [43] (once the spontaneous emission is described properly) and grating-based lasers [44], [45], which are usually computationally demanding for robust numerical solvers. In the framework of the proposed formalism, the variations in the parameters of photonic crystal or grating and consequently the time-dependent performance can be studied semi-analytically. Another example are the lasers based on liquid crystals, in which generally time-dependent external fields can induce and modify optical anisotropies within the cavity [46], [47]. Such effects can be described using the proposed theory of anisotropy rates. Alternatively, its the diamond Raman laser, in which the gain and birefringence principal axes are not collinear, as reported recently [48], and for which our approach can provide a clear recipe to derive the polarization-resolved rate equations with nonlinearities.

In the near future, the work introduced in this paper can be directly used in order to study the properties of spin-injected VCSELs with highly-birefringent gratings for ultrafast applications. Moreover, our results indicate that the presence of both

circular and linear anisotropy in spin-VCSELs together with their 2-mode emission regime makes them interesting candidates for studying aspects of non-Hermitian physics by means of polarization dynamics. Furthermore, this work can motivate the development of more sophisticated perturbative tools, following the trends of non-Hermitian photonics and cavity perturbation theories which correctly describe also the effects due to perturbations of cavity boundaries.

Appendix A
Theory of Effective Loss Field $\tilde{\kappa}$

Using the notation and definitions introduced in this work, the local loss field $\tilde{\kappa}(\mathbf{r},\omega_j)$ is equal to [25]:

$$\begin{aligned}\tilde{\kappa}(\mathbf{r},\omega_j) &= \tilde{\kappa}_{tr}(\mathbf{r},\omega_j) + \tilde{\kappa}_{abs}(\mathbf{r},\omega_j)\\ &= ic\sqrt{\varepsilon(\mathbf{r},\omega_j)}\,\mathbf{n}_s(\mathbf{r})\delta(\mathbf{r}-\mathbf{r}_s)\frac{1}{q_j(\mathbf{r},\omega_j)}\nabla\\ &\quad + \omega_j\,\varepsilon_i(\mathbf{r},\omega_j).\end{aligned} \tag{32}$$

It consists of the Fresnel (transmission) contribution $\tilde{\kappa}_{tr}(\mathbf{r},\omega_j)$ and the intra-cavity absorption $\tilde{\kappa}_{abs}(\mathbf{r},\omega_j)$. Symbol $\mathbf{r}_s$ is the output cavity surface coordinate vector in the media surrounding the cavity, $\mathbf{n}_s(\mathbf{r})$ is the normal surface vector normalized to unity and $q_j(\mathbf{r},\omega_j)$ is the absolute value of wave-number of jth mode. Having already compared the $\tilde{\kappa}_{abs}$ contribution to the well-established computational methods in Ref. [25], we now demonstrate the correctness of the $\tilde{\kappa}_{tr}$ formula. Assuming a simple one-dimensional cavity surrounded by air, we have

$$\kappa_{tr} = \frac{c\,|\varphi(z_s)|^2}{[\varphi|\varepsilon(z,\omega)|\varphi]_C} \tag{33}$$

and z_s stands for the coordinate at the boundary between cavity and air. Such analytic formula expresses the well-known result, that Fresnel losses of the given mode are proportional to the ratio of the integrated absolute value of the Poynting vector to total mode volume. We consider a symmetric λ-cavity with Bragg reflectors made of N_B units of GaAs/AlAs and optimized for $\lambda = 940\,\text{nm}$. The calculated photon lifetime τ_{ph} of the cavity considering several values of N_B is depicted in Fig. 6 demonstrating perfect agreement with the results of the rigorous method based on the transfer matrix formalism. The present method allows to evaluate a photon lifetime using the mode shapes.

Appendix B
Improved Formulation of Anisotropy Operator $\hat{\gamma}$

We have considered the frequency-degenerate basis in Ref. [25] in which the anisotropy operator was introduced in a rather complicated way. Considering the improvement in the formulation of the problem in this work, we show a more elegant way to introduce the anisotropy operator. Let us express the wave equation in SVEA as:

$$\begin{aligned}\varepsilon(\mathbf{r},\omega)\frac{\partial}{\partial t}\mathbf{E}(\mathbf{r},t) = &-\frac{\tilde{\kappa}(\mathbf{r},\omega)}{2}\mathbf{E}(\mathbf{r},t) - i\frac{\omega}{2\varepsilon_0}\tilde{\mathbf{P}}(\mathbf{r},t)\\ &-\hat{\gamma}(\mathbf{r},\omega)\mathbf{E}(\mathbf{r},t).\end{aligned} \tag{34}$$

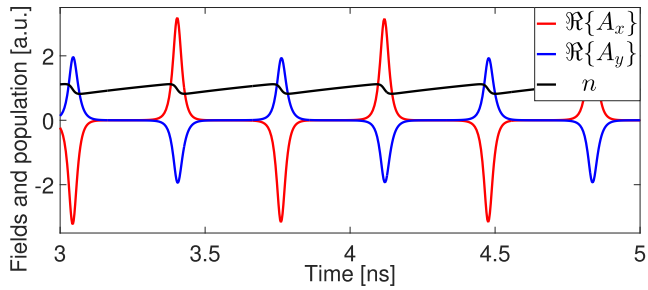

(a)

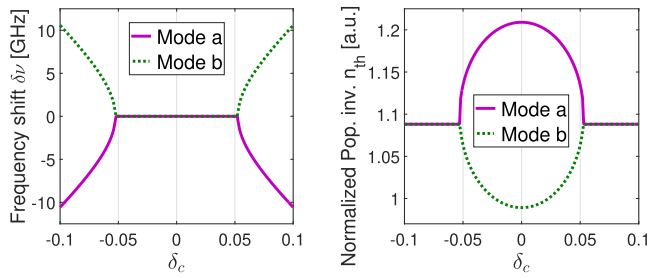

(b)

Fig. 5. Calculated (a) time-dependence of real parts of field amplitudes A_{x, y} and population inversion n for $\delta_g = 0.1$, $\delta_l = 0$ and $\delta_c = 0 : 045$ with constant pumping rate n_0 twice above the threshold value and (b) the frequency shifts δv and population inversions n_{th} of both modes, indicating the presence of EPs.

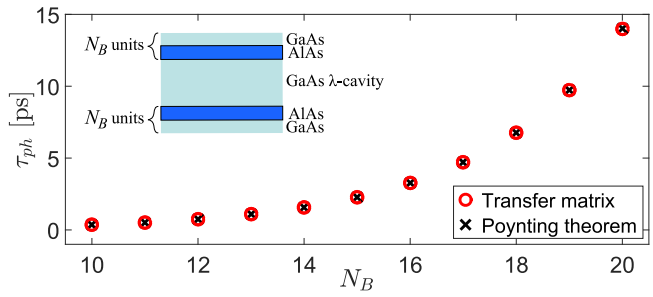

Fig. 6. Photon lifetime $\tau_{ph} = 1/(2\kappa_{tr})$ as a function of the number N_B of GaAs/AlAs units of the cavity Bragg reflectors. Semi-analytic calculation based on the Poynting theorem (black crosses) perfectly agrees with the transfer matrix calculations (red circles).

The modified anisotropy operator $\hat{\gamma}(\mathbf{r},\omega)$ is introduced in (34):

$$\hat{\gamma}(\mathbf{r},\omega) = i\frac{\omega}{2}\hat{\varepsilon}(\mathbf{r},\omega) + i\frac{c^2}{2\omega}\hat{1}\nabla^2. \tag{35}$$

The most important advantage of such expression is the absence of inverse of the permittivity tensor, which was additionally in product with Laplace operator ∇^2 in original work [25].

It can be shown that for the simple cases of plane waves the anisotropy operator can be replaced as follows:

$$\hat{\gamma}'(\mathbf{r},\omega) = i\frac{\omega}{2}\hat{\varepsilon}(\mathbf{r},\omega) - i\frac{c^2}{2\omega}\mathbf{q}^2(\mathbf{r},\omega)\hat{1}; \tag{36}$$

similarly as it was done by Mulet *et al.* [18], where $\mathbf{q}(\mathbf{r},\omega)$ is the wave-vector. However, the authors assumed there the effective homogeneous cavity of a VCSEL. Finally, it can be shown that

for the most of the practical cases $\hat{\gamma}(\mathbf{r},\omega)$ reduces to:

$$\hat{\gamma}''(\mathbf{r},\omega) = i\frac{\omega}{2}\delta\hat{\varepsilon}(\mathbf{r},\omega). \tag{37}$$

This is a very simple and intuitive expression for the anisotropy operator, indicating the possible connection with the cavity perturbation theories.

Appendix C
Beyond The Two-Level Atom Approximation (Class-B Lasers)

Some classes of lasers, especially the semiconductor-based devices, cannot be described with sufficient precision in the framework of standard two-level atom approximation. It means that their unsaturated gain does not have a linear dependence on population inversion as predicted by two-level Maxwell-Bloch equations. In the following, we show, how to apply the present formalism to lasers with nonlinear dependence of gain on population inversion (or carrier concentration in the context of semiconductor photonics). The approach is demonstrated for the cases, in which the polarization vectors of laser modes are spatially independent and gain medium dipole moment densities follow adiabatically the electric field. Furthermore, we assume, that particular optical transitions are not coupled, which can be further studied in the near future.

The eliminated dipole moment density $\tilde{\mathbf{P}}_\mu(\mathbf{r},t)$ reads:

$$\tilde{\mathbf{P}}_\mu(\mathbf{r},t) = i\varepsilon_0\hat{\chi}_\mu[N_\mu(\mathbf{r},t)]\,\mathbf{E}(\mathbf{r},t), \tag{38}$$

where $\hat{\chi}_\mu[N_\mu(\mathbf{r},t)]$ is the susceptibility tensor, which is generally a complicated function of carrier concentrations and dipole moment operator. Let us expand $\hat{\chi}_\mu[N_\mu(\mathbf{r},t)]$ into the $N_\mu(\mathbf{r},t)$-dependent polynomial series as [49]:

$$\hat{\chi}_\mu[N_\mu(\mathbf{r},t)] = \hat{\chi}_\mu^{(0)} + \hat{\chi}_\mu^{(1)}N_\mu(\mathbf{r},t) + \frac{1}{2}\hat{\chi}_\mu^{(2)}N_\mu^2(\mathbf{r},t) + \ldots \tag{39}$$

in which the series tensor coefficients $\hat{\chi}_\mu^{(p)} = \chi_\mu^{(p)}\hat{\mathcal{T}}_\mu^{(p)}$ of pth order are defined.

For the purpose of clarity, let us consider only linear and quadratic terms of N of the series. The derived expressions can be later extended straightforwardly for an arbitrary order of the series. Equation (38) with linear and quadratic terms can be expressed using bra-ket notation as:

$$|\tilde{P}_\mu(t)\rangle = i\varepsilon_0\left[\hat{\chi}_\mu^{(1)}N_\mu(\mathbf{r},t) + \frac{1}{2}\hat{\chi}_\mu^{(2)}N_\mu^2(\mathbf{r},t)\right]|E(t)\rangle. \tag{40}$$

One can notice, that the second-order terms may lead to difficulties, when we decide to perform the derivation of coupled-mode equations by projecting the equation onto $\langle j|$. This can be solved by introducing the identity operator $\hat{I}$:

$$\hat{I} = \sum_k |k\rangle\langle k|. \tag{41}$$

Using the identity operator $\hat{I}$, the quadratic term becomes $N_\mu^2(\mathbf{r},t) \to N_\mu(\mathbf{r},t)\hat{I}N_\mu(\mathbf{r},t)$. It is important to note, that such expressions are meaningful only under the integral.

Employing the recipe from Sec. III and decomposing the basis functions into their polarization and spatial parts: $|k\rangle = \mathbf{e}_k|k]$, we derive:

$$\tilde{P}_{\mu,j}(t) = i\frac{\varepsilon_0}{\mathcal{A}_j}\sum_l \chi_\mu^{(1)}\mathcal{N}_\mu^{jl}(t)\mathcal{T}_{\mu,jl}^{(1)}E_l(t)f_{lj}(t) + i\frac{\varepsilon_0}{\mathcal{A}_j}\sum_{k,l}\frac{\chi_\mu^{(2)}}{2}\mathcal{N}_\mu^{jk}(t)\mathcal{N}_\mu^{kl}(t)\mathcal{T}_{\mu,jl}^{(2)}E_l(t)f_{lj}(t), \tag{42}$$

where the population overlaps are now defined as follows $\mathcal{N}_\mu^{jk}(t) = [j|N_\mu(\mathbf{r},t)|k]$, which is the consequence of the assumption that the gain medium background permittivity is constant withing its volume. Furthermore, the optical gain tensor matrix elements are defined according to $\mathcal{T}_{\mu,jk}^{(p)} = \mathbf{e}_j^\dagger\hat{\mathcal{T}}_\mu^{(p)}\mathbf{e}_k$. For simplicity, we assumed $\langle j||k\rangle_A = \delta_{jk}\mathcal{A}_k$.

Acknowledgment

The authors would like to thank Tomasz Czyszanowski for fruitful discussions on physics of microcavities.

References

[1] W. M. Doyle and M. B. White, "Effects of atomic degeneracy and cavity anisotropy on the behavior of a gas laser," *Phys. Rev.*, vol. 147, pp. 359–367, Jul. 1966.
[2] W. E. Lamb, "Theory of an optical maser," *Phys. Rev.*, vol. 134, pp. A1429–A1450, Jun. 1964.
[3] W. van Haeringen, "Polarization properties of a single-mode operating gas laser in a small axial magnetic field," *Phys. Rev.*, vol. 158, pp. 256–272, Jun. 1967.
[4] M. Sargent, W. E. Lamb, and R. L. Fork, "Theory of a Zeeman laser. I," *Phys. Rev.*, vol. 164, pp. 436–449, Dec. 1967.
[5] M. Sargent, W. E. Lamb, and R. L. Fork, "Theory of a Zeeman laser. II," *Phys. Rev.*, vol. 164, pp. 450–465, Dec. 1967.
[6] D. Lenstra, "On the theory of polarization effects in gas lasers," *Phys. Rep.*, vol. 59, no. 3, pp. 299–373, 1980.
[7] M. V. Tratnik and J. E. Sipe, "Stokes vectors and polarization lasers," *J. Opt. Soc. Amer. B*, vol. 2, no. 10, pp. 1690–1695, Oct. 1985.
[8] M. V. Tratnik and J. E. Sipe, "Polarization eigenstates of a Zeeman laser," *J. Opt. Soc. Amer. B*, vol. 3, no. 8, pp. 1127–1137, Aug. 1986.
[9] P. Paddon, E. Sjerve, A. D. May, M. Bourouis, and G. Stéphan, "Polarization modes in a quasi-isotropic laser: A general anisotropy model with applications," *J. Opt. Soc. Amer. B*, vol. 9, no. 4, pp. 574–589, Apr. 1992.
[10] M. San Miguel, Q. Feng, and J. V. Moloney, "Light-polarization dynamics in surface-emitting semiconductor lasers," *Phys. Rev. A*, vol. 52, pp. 1728–1739, Aug. 1995.
[11] J. Martin-Regalado, F. Prati, M. S. Miguel, and N. B. Abraham, "Polarization properties of vertical-cavity surface-emitting lasers," *IEEE J. Quantum Electron.*, vol. 33, no. 5, pp. 765–783, May 1997.
[12] M. Travagnin, M. P. van Exter, A. K. Jansen van Doorn, and J. P. Woerdman, "Role of optical anisotropies in the polarization properties of surface-emitting semiconductor lasers," *Phys. Rev. A*, vol. 54, pp. 1647–1660, Aug. 1996.
[13] M. Travagnin, "Linear anisotropies and polarization properties of vertical-cavity surface-emitting semiconductor lasers," *Phys. Rev. A*, vol. 56, pp. 4094–4105, Nov. 1997.
[14] S. Balle, E. Tolkachova, M. S. Miguel, J. R. Tredicce, J. Martín-Regalado, and A. Gahl, "Mechanisms of polarization switching in single-transverse-mode vertical-cavity surface-emitting lasers: Thermal shift and nonlinear semiconductor dynamics," *Opt. Lett.*, vol. 24, no. 16, pp. 1121–1123, Aug. 1999.
[15] T. Fördös *et al.*, "Eigenmodes of spin vertical-cavity surface-emitting lasers with local linear birefringence and gain dichroism," *Phys. Rev. A*, vol. 96, Oct. 2017, Art. no. 043828.
[16] T. Fördös, K. Postava, H. Jaffrès, D. Quang To, J. Pištora, and H. J. Drouhin, "Mueller matrix ellipsometric study of multilayer spin-VCSEL structures with local optical anisotropy," *Appl. Phys. Lett.*, vol. 112, no. 22, 2018, Art. no. 221106.

[17] D. Burak, J. V. Moloney, and R. Binder, "Microscopic theory of polarization properties of optically anisotropic vertical-cavity surface-emitting lasers," *Phys. Rev. A*, vol. 61, Apr. 2000, Art. no. 053809.
[18] J. Mulet and S. Balle, "Spatio-temporal modeling of the optical properties of VCSELs in the presence of polarization effects," *IEEE J. Quantum Electron.*, vol. 38, no. 3, pp. 291–305, Mar. 2002.
[19] M. S. Torre, C. Masoller, and P. Mandel, "Transverse and polarization effects in index-guided vertical-cavity surface-emitting lasers," *Phys. Rev. A*, vol. 74, Oct. 2006, Art. no. 043808.
[20] A. Valle, M. Sciamanna, and K. Panajotov, "Nonlinear dynamics of the polarization of multitransverse mode vertical-cavity surface-emitting lasers under current modulation," *Phys. Rev. E*, vol. 76, Oct. 2007, Art. no. 046206.
[21] S. E. Hodges, M. Munroe, J. Cooper, and M. G. Raymer, "Multimode laser model with coupled cavities and quantum noise," *J. Opt. Soc. Amer. B*, vol. 14, no. 1, pp. 191–199, Jan. 1997.
[22] S. V. Zhukovsky, D. N. Chigrin, and J. Kroha, "Bistability and mode interaction in microlasers," *Phys. Rev. A*, vol. 79, Mar. 2009, Art. no. 033803.
[23] O. Malik, K. G. Makris, and H. E. Türeci, "Spectral method for efficient computation of time-dependent phenomena in complex lasers," *Phys. Rev. A*, vol. 92, Dec. 2015, Art. no. 063829.
[24] R. Paquet *et al.*, "Coherent continuous-wave dual-frequency high-Q external-cavity semiconductor laser for GHz-THz applications," *Opt. Lett.*, vol. 41, no. 16, pp. 3751–3754, Aug. 2016.
[25] M. Drong *et al.*, "Spin-VCSELs with local optical anisotropies: Toward terahertz polarization modulation," *Phys. Rev. Appl.*, vol. 15, Jan. 2021, Art. no. 014041.
[26] A. Siegman, *Lasers*. Sausalito, CA, USA: University Science Books, 1986.
[27] M. Sargent, M. O. Scully, and W. E. Lamb, *Laser Physics*. London, U.K.: Addison-Wesley, 1974.
[28] H. Haken, *Light II: Laser Light Dynamics*. Amsterdam, The Netherlands: North Holland, 1985.
[29] H. Fu and H. Haken, "Semiclassical dye-laser equations and the unidirectional single-frequency operation," *Phys. Rev. A*, vol. 36, pp. 4802–4816, Nov. 1987.
[30] H. E. Türeci, A. D. Stone, and B. Collier, "Self-consistent multimode lasing theory for complex or random lasing media," *Phys. Rev. A*, vol. 74, Oct. 2006, Art. no. 043822.
[31] L. Ge, Y. D. Chong, and A. D. Stone, "Steady-state ab initio laser theory: Generalizations and analytic results," *Phys. Rev. A*, vol. 82, Dec. 2010, Art. no. 063824.
[32] S. Esterhazy *et al.*, "Scalable numerical approach for the steady-state *ab initio* laser theory," *Phys. Rev. A*, vol. 90, Aug. 2014, Art. no. 023816.
[33] W. Cartar, J. Mørk, and S. Hughes, "Self-consistent Maxwell-Bloch model of quantum-dot photonic-crystal-cavity lasers," *Phys. Rev. A*, vol. 96, Aug. 2017, Art. no. 023859.
[34] M. Lindemann *et al.*, "Ultrafast spin-lasers," *Nature*, vol. 568, pp. 1–4, 2019.
[35] P. Lalanne, W. Yan, K. Vynck, C. Sauvan, and J.-P. Hugonin, "Light interaction with photonic and plasmonic resonances," *Laser Photon. Rev.*, vol. 12, no. 5, 2018, Art. no. 1700113.
[36] M. Dems, R. Kotynski, and K. Panajotov, "Planewave admittance method - A novel approach for determining the electromagnetic modes in photonic structures," *Opt. Exp.*, vol. 13, no. 9, pp. 3196–3207, May 2005.
[37] A. Brejnak *et al.*, "Boosting the output power of large-aperture lasers by breaking their circular symmetry," *Optica*, vol. 8, no. 9, pp. 1167–1175, Sep. 2021.
[38] A. Joly *et al.*, "Compensation of the residual linear anisotropy of phase in a vertical-external-cavity-surface-emitting laser for spin injection," *Opt. Lett.*, vol. 42, no. 3, pp. 651–654, Feb. 2017.
[39] M. Alouini, J. Frougier, A. Joly, G. Baili, D. Dolfi, and J.-M. George, "VSPIN: A new model relying on the vectorial description of the laser field for predicting the polarization dynamics of spin-injected V(E)CSELs," *Opt. Exp.*, vol. 26, no. 6, pp. 6739–6757, Mar. 2018.
[40] B. R. Cemlyn *et al.*, "Polarization responses of a solitary and optically injected vertical cavity spin laser," *IEEE J. Quantum Electron.*, vol. 55, no. 6, pp. 1–9, Dec. 2019, Art. no. 2400409.
[41] M.-A. Miri and A. Alù, "Exceptional points in optics and photonics," *Science*, vol. 363, no. 6422, 2019, Art. no. eaar7709.
[42] K. Hirose, Y. Liang, Y. Kurosaka, A. Watanabe, T. Sugiyama, and S. Noda, "Watt-class high-power, high-beam-quality photonic-crystal lasers," *Nature Photon.*, vol. 8, pp. 406–411, 2014.
[43] A. Y. Song, A. R. K. Kalapala, W. Zhou, and S. Fan, "First-principles simulation of photonic crystal surface-emitting lasers using rigorous coupled wave analysis," *Appl. Phys. Lett.*, vol. 113, no. 4, 2018, Art. no. 041106.
[44] T. Pusch *et al.*, "Vertical-cavity surface-emitting laser with integrated surface grating for high birefringence splitting," *Electron. Lett.*, vol. 55, no. 19, pp. 1055–1057, 2019.
[45] T. Fördös *et al.*, "Quantum dot-based optically pumped VCSELs with high-contrast periodic gratings," in *Proc. 24th Microopt. Conf.*, Nov. 2019, pp. 306–307.
[46] Y. Matsuhisa, R. Ozaki, Y. Takao, and M. Ozaki, "Linearly polarized lasing in one-dimensional hybrid photonic crystal containing cholesteric liquid crystal," *J. Appl. Phys.*, vol. 101, no. 3, 2007, Art. no. 033120.
[47] G. E. Nevskaya, S. P. Palto, and M. G. Tomilin, "Liquid-crystal-based microlasers," *J. Opt. Technol.*, vol. 77, no. 8, pp. 473–486, Aug. 2010.
[48] O. Kitzler, D. J. Spence, and R. P. Mildren, "Generalised theory of polarisation modes for resonators containing birefringence and anisotropic gain," *Opt. Exp.*, vol. 27, no. 12, pp. 17209–17220, Jun. 2019.
[49] M. Sargent, "Theory of a multimode quasiequilibrium semiconductor laser," *Phys. Rev. A*, vol. 48, pp. 717–726, Jul. 1993.